JCB Report

Stored elastic energy powers the 60-μm extension of the *Limulus polyphemus* sperm actin bundle

Jennifer H. Shin,[1] L. Mahadevan,[4] Guillermina S. Waller,[5] Knut Langsetmo,[6] and Paul Matsudaira[2,3,5]

[1]Department of Mechanical Engineering, [2]Department of Biology, and [3]Division of Biological Engineering, Massachusetts Institute of Technology, Cambridge, MA 02139
[4]Department of Applied Mathematics and Theoretical Physics, University of Cambridge, CB3 9EW, Cambridge, UK
[5]Whitehead Institute for Biomedical Research, Cambridge, MA 02142
[6]Boston Biomedical Research Institute, Watertown, MA 02472

During the 5 s of the acrosome reaction of *Limulus polyphemus* sperm, a 60-μm-long bundle of scruin-decorated actin filaments straightens from a coiled conformation and extends from the cell. To identify the motive force for this movement, we examined the possible sources of chemical and mechanical energy and show that the coil releases ~10^{-13} J of stored mechanical strain energy, whereas chemical energy derived from calcium binding is ~10^{-15} J. These measurements indicate that the coiled actin bundle extends by a spring-based mechanism, which is distinctly different from the better known polymerization or myosin-driven processes, and that calcium initiates but does not power the reaction.

Introduction

The acrosome reaction of the sperm of the horseshoe crab *Limulus polyphemus* is an unusual example of actin-based motility. Upon contact with the egg jelly coat, a bundle of actin filaments cross-linked by scruin–CaM heterodimers extends from the head of the sperm through a nuclear channel to form a 60-μm-long finger of membrane, the acrosomal process. The reaction requires the presence of Ca^{2+} ions and is completed in ~5 s. However, because the bundle is preformed as a coil around the base of the nucleus and does not contain myosin, extension of the membrane must involve a different mechanism for generating force than polymerization or molecular motor-based processes. Based on structural analysis of the actin bundle before and after activation, DeRosier et al. (1982) suggested that the movement was driven by a spring-like mechanism in which mechanical energy is stored in the conformation of the coiled bundle.

The structure of the coiled bundle is unlike any known actin structure (Fig. 1). In contrast to the typical linear conformation of actin bundles in microvilli or filopodia, the coiled state consists of six polygonal loops. Each loop is made of 14 straight segments connected by kinks at 0.7-μm intervals (DeRosier et al., 1980). In addition to the polygonal structure of the bundle, the bundle exhibits a 60° superhelical twist per segment, which gives rise to 14–15 revolutions along the entire bundle, thus, allowing different filaments to cover equivalent distances in a coil. This macroscopic helical packing conformation arises due to the small microscopic overtwist of 0.23° per each subunit, and is putatively the basis for storing energy and driving the extension of the bundle (DeRosier and Tilney, 1984). The small difference in twist between subunits, which represents a relatively large twisting strain τ of ~85.4°/μm (DeRosier et al., 1980) is amplified by the polymeric assembly of the filament into almost two additional turns over the 10^6 subunits along the length of the bundle. During the acrosome reaction, the filaments untwist, bends melt, and the coil rotates and straightens to a true discharge (TD) state (DeRosier et al., 1980, 1982). The change in actin twist coupled to the uncoiling of the polygonal bundle is postulated to be the motive force for extension of the bundle.

Results and discussion

To understand how the acrosomal process extends, we examined the relative contributions of the mechanical and chemical potentials to the free energy change that accompanies the reaction. First, we estimate the stored elastic strain energy in

The online version of this article includes supplemental material.

Address correspondence to L. Mahadevan, Department of Applied Mathematics and Theoretical Physics, University of Cambridge, CB3 0WA, Cambridge, UK. Tel.: 44-1223-766-891. Fax: 44-1223-765-900. email: l.mahadevan@damtp.cam.ac.uk

Key words: acrosomal reaction; mechanical spring; calcium energy; calorimetry

Abbreviations used in this paper: FD, false discharge; TD, true discharge.

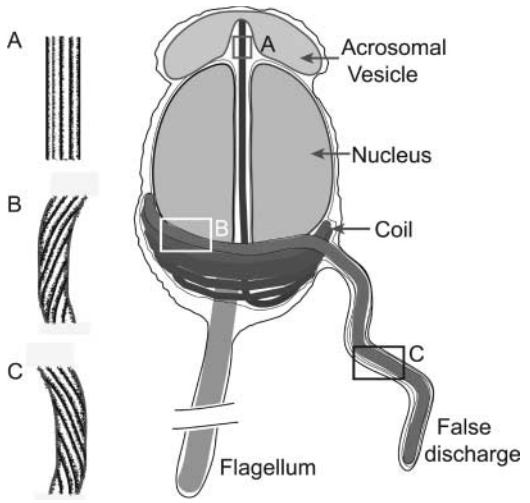

Figure 1. **A schematic of *Limulus* sperm based on electron micrographs.** The filaments are twisted in the coiled state and the FD state with opposite chirality but straight in the TD state. During the acrosomal reaction, the actin filaments untwist and unbend going from the coil to the TD. Sometimes the unbending does not occur, leading to kinked TDs (see Fig. S1, available at http://www.jcb.org/cgi/content/full/jcb.200304006/DC1).

the twisted bundle by treating it as an initially straight, isotropic, elastic rod of circular cross section (the hexagonal packing of the filaments allows this as a reasonable first approximation) that is uniformly twisted. For such a rod, the elastic stored energy is (Landau and Lifshitz, 1986):

$$U \approx \int_0^L \frac{1}{2}(A\kappa^2 + C\tau^2)ds, \quad (1)$$

where A is the bending stiffness, κ is the curvature of the bundle, C is the twisting stiffness, τ is the twist per unit length, and L is the total length of the bundle. Based on this relationship, we can estimate the stored energy with the measured values of the bending and twisting stiffness.

Electron micrographs reveal that the bundle is sharply bent at 0.7-μm intervals (see Fig. S1, available at http://www.jcb.org/cgi/content/full/jcb.200304006/DC1). The large curvature about the kinks extends over a length of the order of the thickness of the bundle; over this distance the filaments slip relative to each other just like in tilt boundaries in crystalline materials (Nabarro, 1967). Because the energy of the kinks scales sublinearly with the length of the bundle, this energy is small.

In contrast to having a discrete number of bends, the coiled bundle is continuously twisted over its length. Because the energy associated with kinks is small, the stored elastic energy in Eq. 1 may then be well approximated by:

$$U \approx C\tau^2 L/2.$$

For an isotropic rod with a circular cross section, $A = 3C/2$, a good estimate of the twisting stiffness C may be derived from the bending stiffness A, which is much easier to measure. We estimate the bending stiffness of the acrosome bundle from the shape of the bent bundle when subjected to a steady hydrodynamic flow at low Reynolds numbers (see Materials and methods), and find it to be $A \approx 5 \times 10^{-21}$ Nm^2 (5×10^9 pN·nm^2), leading to a persistence length of $l_p \approx A/k_BT \approx 1.2$ m. The total stored elastic energy in twist is then $U \approx A\tau^2 L/3 \approx 3 \times 10^{-13}$ J (7×10^7 k_BT), and is much larger than the energy in the kinks. Indeed, the kinks are important only geometrically; they pack the bundle into the sperm in an energetically efficient manner and convert twist into extension during unpacking (DeRosier and Tilney, 1984). Evidence of this is seen in experiments (see Fig. S1, available at http://www.jcb.org/cgi/content/full/jcb.200304006/DC1), where the kinks sometimes do not melt leading to a kinked TD. Thus, the acrosome reaction can be thought of as a two-step process: (1) the primary event, wherein the bundle untwists and extends, with the kinks converting (un)twist to extension; and (2) the secondary event, wherein the kinks melt, though this does not always have to follow.

Although mechanical energy is clearly responsible for large movements of macromolecular assemblies, energy may also be contributed by two other obvious energy sources, hydrolysis of ATP by actin and the energy released by Ca^{2+} binding. In a typical filament, the bound nucleotide in an actin subunit is ADP. However, it is conceivable that delayed hydrolysis of ATP could be coupled to extension of the bundle. Thus, we determined the state of bound nucleotide in the false discharge (FD) form (Fig. 1) of the acrosomal bundle by ion exchange column chromatography (see Materials and methods). The nucleotide status of the FD is measured for two reasons. First, the coiled bundles cannot be purified with any degree of biochemical purity and isolated coils are always contaminated with small fragments of FD. Second, the FD is a valid model of the coil because the two forms are rapidly and reversibly interconvertible in live cells (Andre, 1965). Because a cell can spontaneously extend and retract a FD within a few minutes, it is unlikely that the coil has a bound nucleotide different than the FD. Based on the elution volumes and peak areas of known amounts of injected nucleotide standards, the extracted nucleotide from both the TD and FD states is ADP (see Materials and methods). ATP is not detected in either preparation. Furthermore, the stoichiometry of extracted ADP to actin is 1.2:1 (mole/mole). Thus, the coiled bundle most likely consists of ADP-actin subunits (Fig. 2).

A second more probable source of chemical energy is the energy released by Ca^{2+} binding to the bundle. From thermodynamics, the energy of Ca^{2+} binding is simply the difference between the energy of binding to the coil and to the TD (Wyman, 1964). The sole Ca^{2+} binding sites in the bundle reside in the single CaM subunit of scruin–CaM heterodimers. To measure Ca^{2+} binding energy, we measured the heat of Ca^{2+} binding to the TD and FD forms of the bundle by isothermal titration calorimetry (see Materials and methods). In control experiments with isolated horseshoe crab CaM and scruin–CaM complexes, Ca^{2+} bound to four sites in the heterodimer. However, in the isolated actin bundle of the TD or FD, only two Ca^{2+} binding sites were detected (Table I). From the heat of binding we derive an association constant and finally a Gibbs free energy. The calculated difference in energy of binding to the FD and TD at 25°C is 3.6×10^{-15} J (8.8×10^5 k_BT). This value, an upper bound on the available free energy of Ca^{2+} binding, is al-

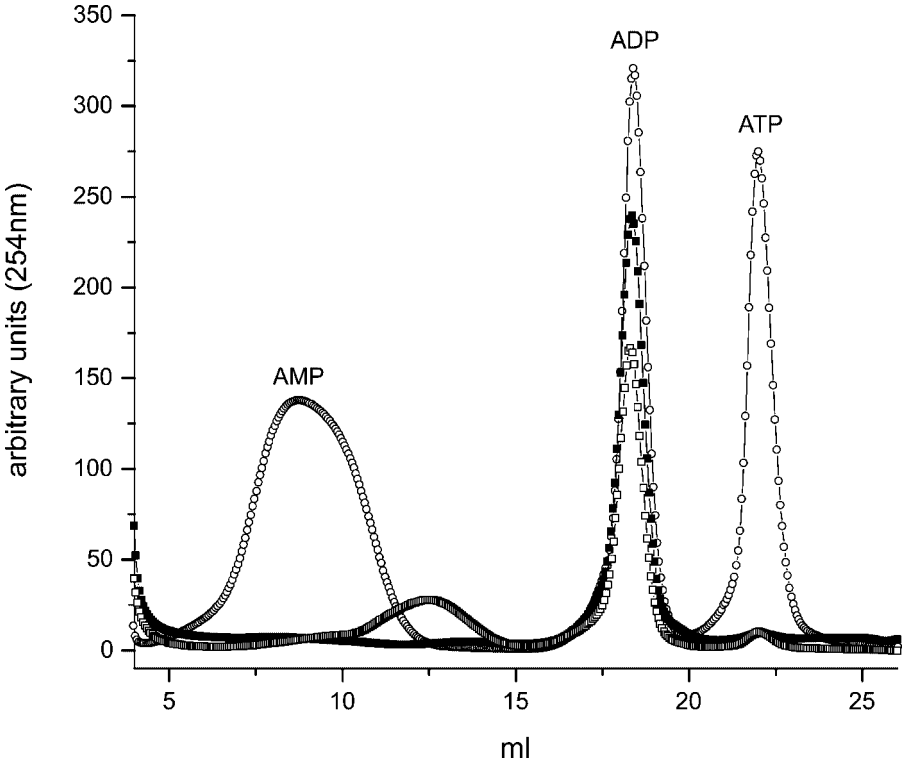

Figure 2. **Chromatographs of nucleotides eluted from an ion exchange column.** AMP, ADP, and ATP display elution volumes of 7, 18.5, and 22 ml. Nucleotides extracted from the true (closed squares) and false (open squares) are identified as predominantly ADP when compared with nucleotide standards (open circles). The minor peak at 12.5 ml is unidentified.

most two orders of magnitude smaller than the lower bound estimate of the elastic energy. Our measurements of sources of mechanical and chemical energy show that there is ample elastic energy to extend the acrosomal process.

Having considered the sources of energy, we now briefly turn to a discussion of the energy sinks in the system. Just as the bundle is able to store a substantial amount of energy in twist, it dissipates this energy as it untwists in a viscous environment. Once the scruin–actin bond is loosened, the untwisting of the filaments leads to shearing between them as is clear from electron micrographs of the different states of the bundle (DeRosier and Tilney, 1984). This leads to a dissipation that can potentially be very large owing to the high degree of confinement that magnifies the shear rate for purely geometric reasons (see Fig. S3, available at http://www.jcb.org/cgi/content/full/jcb.200304006/DC1).

As the bundle extends, it experiences friction in the highly viscous environment. The nuclear channel is very narrow, and the clearance between the channel wall and the bundle surface is only of the order of a few nanometers, whereas the average diameter of the bundle is ~100 nm. Due to this small clearance between the bundle and the channel wall, hydrodynamic dissipation outside the channel is much smaller than the dissipation in the channel. The latter hydrodynamic dissipation rate, $\dot{E}$, is calculated to be 4×10^{-17} W ($10^4\ k_BT/s$) (see Fig. S2, available at http://www.jcb.org/cgi/content/full/jcb.200304006/DC1). Because the duration of the reaction is typically ~5 s, the total energy dissipated is $\dot{E} \approx 10^{-15}$ J ($2.4 \times 10^5\ k_BT$). It must be emphasized that this estimate of dissipated energy, which is nearly three orders of magnitude smaller than the estimated stored elastic energy, provides only a lower bound on the energy required to drive the reaction. Because the velocity of uncoiling changes by nearly an order of magnitude when the temperature is changed by <15%, the rate-limiting step cannot be the viscous resistance of the nuclear channel. Energy may also be consumed as the acrosomal bundle pushes or stretches the membrane during the reaction. However,

Table I. **Thermodynamic parameters for Ca^{2+} binding determined by isothermal titration calorimetry**

Protein	K_1	ΔH_1	K_2	ΔH_2	K_3	ΔH_3	K_4	ΔH_4
	$M^{-1} \times 10^6$	kcal· mol^{-1}	$M^{-1} \times 10^6$	kcal· mol^{-1}	$M^{-1} \times 10^5$	kcal· mol^{-1}	$M^{-1} \times 10^3$	kcal· mol^{-1}
CaM	0.36 ± 0.18	−1.6 ± 0.5	0.16 ± 0.05	0.3 ± 0.7	0.26 ± 0.09	−4.5 ± 0.5	6.1 ± 4.4	−1.8 ± 1.0
Scruin	2.4 ± 0.6	−1.9 ± 0.8	1.9 ± 0.4	−2.9 ± 0.2	2.1 ± 0.2	1.9 ± 0.3	3.2[a]	−1.8 ± 0.5
TD	1.7 ± 0.8	2.5 ± 0.4	1.7 ± 0.8	−2.5 ± 0.4	NO	NO	NO	NO
FD	2.5 ± 0.4	−3.1 ± 0.1	2.5 ± 0.4	−3.1 ± 0.1	NO	NO	NO	NO

K and ΔH for the binding of each Ca^{2+} are determined by a nonlinear least squares fit of the data. For *Limulus* sperm calmodulin (CaM) and scruin data are fit using a sequential binding model with four sites. Averages and deviations for five (CaM) and two (scruin) experiments are presented. For true discharge (TD) and false discharge (FD), the two high affinity Ca^{2+} binding sites do not have different thermal properties, and were, therefore, fit using a single site model with a stoichiometry of two. Averages and deviations for three (TD) and two (FD) experiments are presented on a per Ca^{2+} basis. Binding of Ca^{2+} to the two low affinity sites of TD and FD was not observed. NO, not observed.

[a]Only the value from one experiment is presented. Fitting for the lowest affinity site was poorly determined in the second dataset.

Tilney (Tilney et al., 1979) showed that the outer nuclear envelope surrounding the coil is converted into the 18 μm^2 of new plasma membrane surrounding the TD. Thus, the membrane is unlikely to be a significant energy sink. We speculate that most of the energy is dissipated by interfilament sliding as the bundle untwists (see Fig. S3, available at http://www.jcb.org/cgi/content/full/jcb.200304006/DC1).

Cellular engines that power motility usually fall into two categories: polymerization ratchets and molecular motors. The work performed by both types of engines depends on continual hydrolysis of ATP. Here, we provide quantitative evidence to support a third type of cellular engine, a spring, in which the energy is stored in the conformation of the actin–scruin complex in the coiled bundle using a subtle combination of geometric packing and chemical binding. We base this conclusion on three pieces of evidence. First, the acrosomal actin bundle is stiff and requires enormous energy to bend and twist into a coil; we estimate the elastic energy to be $\sim 10^{-13}$ J ($2.5 \times 10^7\ k_BT$). To place this number in perspective, we compare the specific power of the acrosome with other force-generating engines. A single bundle contains 10^6 subunits of actin and scruin and a mass $\sim 2 \times 10^{-16}$ kg (Sanders et al., 1996) so that the specific power is 2.5×10^2 J/s kg. This value is two orders of magnitude smaller than the specific power of an ATP-driven motor protein and of the same order of magnitude as the bacterial rotary motor, striated muscle, and a gasoline automobile engine (Mahadevan and Matsudaira, 2000), suggesting that it has sufficient power as a cellular engine for motility. Second, a typical actin-based engine requires expenditure of chemical energy to do work (Lymn and Taylor, 1971). However, we rule out the possibility that ATP hydrolysis is directly coupled to the acrosome reaction because the FD and TD contain ADP in a 1:1 molar ratio with actin. Because the coil can reversibly convert into a FD, the bound nucleotide of the coil is most likely ADP. The third piece of evidence is the low yield of work from Ca^{2+} binding. Although the energy from ligand binding could power the movement, our measurements show that the energy released from Ca^{2+} binding to the TD and FD is insufficient by two orders of magnitude to account for the mechanical energy expended in the reaction. Thus, based on our measurements of mechanical and chemical energy, we conclude that there is ample elastic energy but not chemical energy to extend the acrosomal process.

How conformational changes store energy is unknown but the stiffness measurements and three-dimensional reconstructions of the TD suggest a possible clue. The EM-derived structure shows that the TD is an extensively cross-linked bundle of actin filaments in which scruin cross-links are spaced along every actin subunit (Schmid et al., 1994; Sherman et al., 1999). In contrast, in a more conventional actin bundle fimbrin cross-linked actin filaments (Tilney et al., 1980; Volkmann et al., 2001), cross-links are spaced 36 nm along an actin filament. The difference in stiffness between the acrosomal bundle and a fimbrin-type bundle arises because they differ in the density of protein cross-links between filaments. Based on the measured bending stiffness and an average bundle radius of $r \approx 50$ nm yields a Young's modulus $E = 4A/R^4 \sim 10^9$ Pa for the composite actin–scruin bundle, comparable to that of a stiff elastomer and similar to that of pure actin filaments (Kojima et al., 1994). The Young's modulus is consistent with the three-dimensional structure of the acrosomal bundle, which is closer to a solid rod of protein than a braid of filaments separated by water-filled space. The close association between neighboring filaments inferred from the mechanical properties and the biochemical studies of scruin suggests that scruin is a latch that holds actin filaments and the acrosomal bundle in their unusual conformations. It also explains how changes to the twist of individual filaments are physically coupled to interfilament shearing during the formation and release of the TD (unpublished data).

Recent structural and biochemical studies (Schmid et al., 1994; Sanders et al., 1996; Sherman et al., 1999) are consistent with the hypothesis that the scruin–CaM complex undergoes a conformation change in the presence of Ca^{2+} allowing the twisted actin filaments to untwist relative to each other. Formally, there are two possibilities for the uncoiling mechanism. In an unzipping model, a spatially localized zone of conformational change propagates between the two phases of the acrosome so that only a segment of the bundle uncoils at one time. In this scenario, which is similar to other polymorphic transitions in supramolecular systems (Hotani, 1980), we expect the actin bundle to extend with a nearly constant velocity. In contrast, a global explosion model involves uncoiling throughout the entire bundle, with the nuclear channel converting the change into motion. In this model, the extension velocity of the acrosome would decrease exponentially with time after a short explosive initial transient. Experimental results indicate that the velocity of extension is constant during the reaction, supporting the model where the local untwisting propagates spontaneously along the bundle once a critical threshold is reached; equivalently, the region remains fixed in space while the bundle moves through this region sequentially uncoiling section by section. Because the energy from Ca^{2+} binding is at least 100-fold lower than the expended mechanical energy, our studies suggest that Ca^{2+} is a trigger that initiates the reaction, which is then self-sustained and driven by the stored elastic energy.

This dynamical event is analogous to a phase transition in a crystalline material (Oosawa and Asakura, 1975), which allows for conformation changes to occur in a localized zone of activity (a defect, dislocation, or front) where the material is transformed from one ordered phase (twisted) to another (untwisted). A simple analogy that illustrates the role of localized zones of activity may be found by considering the motion of a heavy carpet on the ground. It can be moved by (a) pulling it so that it slides uniformly, or (b) by forming a small localized fold that is then forced to roll along the carpet. Clearly, the latter is energetically more efficient, but requires some energy to nucleate a fold before it can propagate under the influence of, say, gravity. Just as in the context of a carpet, a critical size of the untwisted phase for the actin bundle must be nucleated by some environmental factors. Our experiments suggest that Ca^{2+} binding triggers the reaction by changing the relative energy of the different states of the bundle. In particular, it makes the initially unstable straight state sta-

ble relative to the coiled state. Once this critical event has occurred, we hypothesize that the reaction proceeds without any further need for Ca^{2+}, and is driven by the stored mechanical energy as the stable phase (the untwisted, unstrained bundle) invades an unstable phase (the twisted, strained bundle). In a long specimen, this front will travel with a nearly constant velocity determined by the balance between the driving force and the dissipation, i.e., the bundle should untwist with a nearly constant velocity. The conversion of twist to extension is achieved in a remarkable way in this system, and uses the presence of kinks (DeRosier and Tilney, 1984; DeRosier et al., 1980; see Fig. S1, available at http://www.jcb.org/cgi/content/full/jcb.200304006/DC1). Thus, the kinks are an efficient way of packing and unpacking the bundle, whereas the twisting strain is an efficient way of storing energy. A quantitative model requires further characterization of the problem parameters, and constitutes work currently in progress (unpublished data).

The coiled *L. polyphemus* acrosomal bundle is not unique in storing elastic energy via small conformation changes in a crystalline protein biopolymer. Other examples include the tubulin assemblies in microtubules, virus capsids and clathrin coats, and bacterial flagella (Oosawa and Asakura, 1975; Yamashita and Namba, 1998; Bray, 2001). In these structures, small changes at the subunit level are amplified by the repetitive polymeric structure into large scale movements. In principle, any polymeric structure is capable of storing elastic energy.

Materials and methods

Sperm and acrosome isolation

Sperm were collected by stimulating the gonopores of *L. polyphemus* males. Cells were centrifuged twice at 750 *g* for 5 min and resuspension in artificial seawater (ASW: 423 mM NaCl, 9 mM KCl, 9.27 mM $CaCl_2$, 22.94 mM $MgCl_2$, 25.5 mM $MgSO_4$, 2.15 mM $NaHCO_3$, and 10 mM Tris, pH adjusted to 8.0) to be stored as a pellet on ice. The TD state was prepared following Sanders et al. (1996). The FD state was prepared following Tilney (1975) but with the minor modification that the FD was induced by suspending the washed sperm in five volumes of 0.1% Triton X-100, 0.1 mM EDTA, 3 mM $MgCl_2$, and 30 mM Tris, pH 8.0 (4°C).

Light microscopy

The acrosome reaction was induced by diluting the sperm suspension with 25 mM $CaCl_2$ to a 1:100 ([vol/vol] $CaCl_2$/ASW). Calcium ionophore A23187 (1 mg/ml in DMSO) was diluted 1:10 with 25 mM $CaCl_2$. The experiments were conducted in a flat capillary flow cell (18 mm × 6 mm × 0.3 mm) constructed from a glass coverslip sealed to a glass microscope slide with Apiezon grease. A sperm suspension was introduced into the flow cell with a pipette and left to adhere to the coverslip. The acrosome reaction was induced with a flow of A23187. Cells were imaged under DIC-H optics at 100× magnification on an inverted microscope (model TE300; Nikon), captured by a video camera (model Orca CCD; Hamamatsu), and digitized at 30 fps using an Apple Video player.

Bending stiffness

Activated sperm cells were adsorbed onto a glass coverslip treated with BIOBOND (EMS, Inc.) and assembled in a flow chamber. Fluid flow was generated by capillary absorption from a filter paper at the opposite to end of the flow chamber. To calculate the velocity of flow, the trajectory of small 0.1-μm-size particles in the fluid were imaged and tracked in the focal plane of the bundle. The bending stiffness was calculated from the profile of digitized images of the bent bundle and the fit to the solution of the differential equation for a rod bent by a hydrodynamic flow (Fig. 3). At these length scales, the dynamics are dominated by viscous effects, and the ratio of inertial to viscous forces, i.e., the Reynolds number (Re), based on the sperm size of 5 μm is Re$\sim 10^{-7}$. For steady flow past the bundle, the equation for the transverse position of the bundle *y(x)* is:

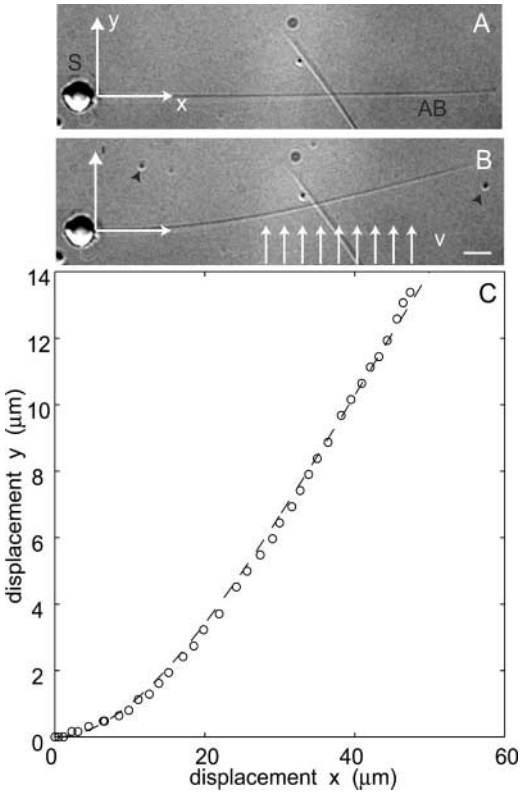

Figure 3. **Measurement of the bending stiffness of the actin bundle.** Shape of the extended acrosome bundle in the absence (A) and the presence (B) of a steady flow. Bar, 5 μm. The trajectory of small 0.1-μm radius particles (two black arrowheads) is used to obtain the velocity of the flow. (C) A theoretical fit to a solution of Eq. 3.

$$A\frac{\partial^4 y}{\partial x^4} + v\zeta = 0, \tag{2}$$

with boundary conditions; at $x = 0$,

$$y = \frac{\partial y}{\partial x} = 0,$$

and at $x = l$,

$$\frac{\partial^3 y}{\partial x^3} = \frac{\partial^2 y}{\partial x^2} = 0,$$

l being the length of the acrosome, v the velocity of the flow measured using bead trajectories. Here, we have used the linearized (small slope) approximation for the elastic behavior of the bundle, and the drag coefficient $\zeta = 4\pi\mu/[\log(l/D)]$, D being the distance of the bundle above the slide (Cox, 1970). We use the shape to determine the average bending stiffness, $A \sim 5 \times 10^{-21}$ Nm^2.

Nucleotide identification

To identify the nucleotide present in the acrosomal process, TD and FD were isolated, washed several times with 50 mM Tris, pH 8.6 (4°C), and dialyzed of free nucleotide. Solid urea was added to washed pellets to a final concentration of 8 M in a final volume of 200 μl to extract the bound nucleotide. Samples were incubated at room temperature for at least 1 h, diluted to 3.2 ml with 50 mM Tris, pH 8.6, and centrifuged at 349,000 *g* for 20 min (Beckman Coulter). The extracts were applied at a flow rate of 0.25 ml/min to a 1-ml TOYOPEARL DEAE-650S ion exchange column equilibrated in 50 mM Tris, pH 8.6. AMP, ADP, and ATP eluted with a gradient of 0–1 M NaCl in 50 mM Tris, pH 8.6. The positions of peaks were monitored at 254 nm and compared with the elution times and peak areas of

AMP, ADP, ATP, GMP, GDP, and GTP nucleotide standards (Sigma-Aldrich) in separate runs under identical conditions. Chromatography was performed at 4°C.

Calorimetry

To measure Ca^{2+} binding to purified acrosomes, trace levels of Ca^{2+} were reduced by washing plasticware and glassware with 1 M HCl. Ca^{2+}-free buffer (150 mM KCl, 25 mM Hepes, pH 7.5, and 3 mM NaN3) was prepared by passing the sample through a CHELEX 100 column. Ca^{2+} was removed from acrosome suspensions by overnight dialysis at 5°C against Ca^{2+}-free buffer containing 0.5% CHELEX 100 resin (200–400 mesh; Bio-Rad Laboratories) and then against two changes of Ca^{2+}-free buffer alone. Ca^{2+} solutions were prepared from a 0.1 M stock solution of a Ca^{2+} standard (Orion) diluted with 150 mM KCl, 25 mM Hepes, pH 7.5, 3 mM NaN_3. Ca^{2+} binding to TD and FD acrosomes was measured by isothermal titration calorimetry using a Microcal VP-ITC instrument. Aliquots of a Ca^{2+} solution, typically 0.25 mM $CaCl_2$ in 150 mM KCl, 25 mM Hepes, pH 7.5, and 3 mM NaN_3 were injected into the calorimetry cell and the heat released was measured. Data was analyzed using Microcal Origin software and was fitted assuming four sequential Ca^{2+} binding sites.

Online supplemental material

Fig. S1 shows the discrete kinks in the coil and illustrates how nature uses kinks to convert the untwisting into the extension of the acrosome. Fig. S2 explains the hydrodynamic dissipation in the nuclear channel during the extension. Finally, a theoretical model for the dynamics of the uncoiling is described in Fig. S3. Online supplemental material is available at http://www.jcb.org/cgi/content/full/jcb.200304006/DC1.

We thank N. Watson for help with imaging. Microscopy was conducted in the W.M. Keck Microscope Facility at the Whitehead Institute.

This work was supported by the Center for Biomedical Engineering at Massachusetts Institute of Technology (to L. Mahadevan and P. Matsudaira); National Institutes of Health supplementary grant (to L. Mahadevan); National Institutes of Health grant GM52703 (to P. Matsudaira); and National Science Foundation Graduate Research Fellowship (to J.H. Shin).

Submitted: 1 April 2003
Accepted: 8 August 2003

References

Andre, J. 1965. A propos d'une lecon sur la limule (I). *Annales de la Faculte des Sciences de l' Universite de Clermont.* 26:27–38.

Bray, D. 2001. Cell Movements. 2nd ed. Garland Publishing, New York. 406 pp.

Cox, R.G. 1970. The motion of long slender bodies in a viscous fluid I. General theory. *J. Fluid Mech.* 44:791–810.

DeRosier, D.J., and L.G. Tilney. 1984. How to build a bend in an actin bundle. *J. Mol. Biol.* 175:57–73.

DeRosier, D.J., L. Tilney, and P. Flicker. 1980. A change in the twist of the actin-containing filaments occurs during the extension of the acrosomal process in *Limulus* sperm. *J. Mol. Biol.* 137:375–389.

DeRosier, D.J., L.G. Tilney, M. Bondar, and P. Frankl. 1982. A change in the twist of actin provides the force for the extension of the acrosomal process in the *Limulus* sperm: the false-discharge reaction. *J. Cell Biol.* 93:324–337.

Hotani, H. 1980. Micro-video study of moving bacterial flagella filaments. II. Polymorphic transition in alcohol. *Biosystems.* 12:325–330.

Kojima, H., A. Ishijima, and T. Yanagida. 1994. Direct measurement of stiffness of single actin filaments with and without tropomyosin by in vitro nanomanipulation, *Proc. Natl. Acad. Sci. USA.* 91:12962–12966.

Landau, L.D., and E.M. Lifshitz. 1986. Theory of Elasticity. 3rd ed. Pergamon, New York. 62 pp.

Lymn, R.W., and E.W. Taylor. 1971. Mechanism of adenosine triphosphate hydrolysis by actomyosin. *Biochemistry.* 10:4617–4624.

Mahadevan, L., and P. Matsudaira. 2000. Motility driven by macromolecular springs and ratchets. *Science.* 288:95–99.

Nabarro, F.R.N. 1967. Theory of Crystal Dislocations. Oxford University Press, Oxford. 821 pp.

Oosawa, F., and S. Asakura. 1975. Thermodynamics of protein polymerization. Academic Press, New York. 204 pp.

Sanders, M., M. Way, J. Sakai, and P. Matsudaira. 1996. Characterization of the actin crosslinking properties of the scruin-CaM complex from the acrosomal process of the *Limulus* sperm. *J. Biol. Chem.* 271:2651–2657.

Schmid, M.F., J.M. Agris, J. Jakana, P. Matsudaira, and W. Chiu. 1994. Three-dimensional structure of a single filament in the *Limulus* acrosomal bundle: scruin binds to homologous helix-loop β motifs in actin. *J. Cell Biol.* 124: 341–350.

Sherman, M.B., J. Jakana, S. Sun, P. Matsudaira, W. Chiu, and M.F. Schmid. 1999. The three-dimensional structure of the *Limulus* acrosomal process—a dynamic actin bundle. *J. Mol. Biol.* 294:139–149.

Tilney, L.G. 1975. Actin filaments in the acrosomal reaction of *Limulus* sperm. *J. Cell Biol.* 64:289–310.

Tilney, L.G., J.G. Clain, and M.S. Tilney. 1979. Membrane events in the acrosomal reaction of *Limulus* sperm. *J. Cell Biol.* 81:229–253.

Tilney, L.G., D.J. DeRosier, and M.J. Mulroy. 1980. The organization of actin filaments in the stereocilia of cochlear hair cells. *J. Cell Biol.* 86:244–259.

Volkmann, N., D. DeRosier, P. Matsudaira, and D. Hanein. 2001. An atomic model of actin filaments cross-linked by fimbrin and its implications for bundle assembly and function. *J. Cell Biol.* 153:947–956.

Wyman, J. 1964. Linked functions and reciprocal effects in hemoglobin: a second look. *Adv. Protein Chem.* 19:223–286.

Yamashita, I., and K. Namba. 1998. Structure and switching of bacterial flagellar filaments studied by X-ray fiber diffraction. *Nat. Struct. Biol.* 5:125–132.

JCB
Online Supplemental Material

Shin et al. http://www.jcb.org/cgi/doi/10.1083/jcb.200304006

Supplemental Figures 1–3.

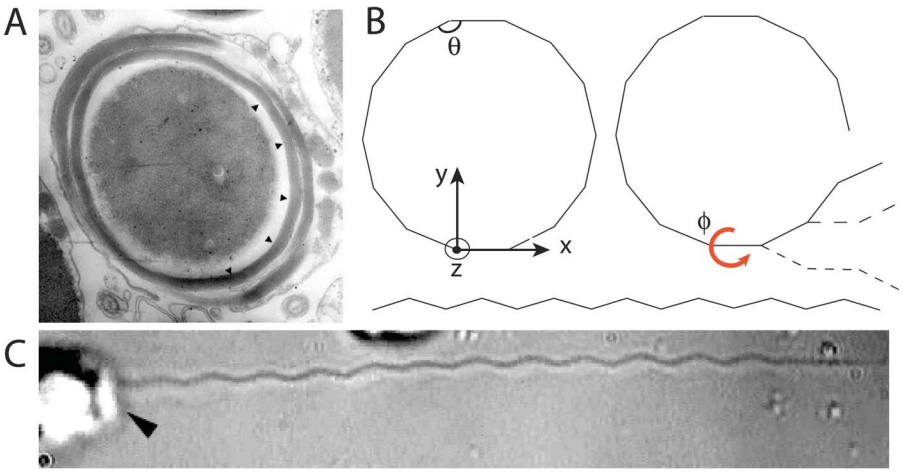

Figure S1. **Uncoiling of bent and twisted rods.** (A) A thin section electron micrograph of a sperm cross-section shows that the bundle is bent discretely (arrowheads) with a series of arms separated by elbows, allowing the 60-μm bundle to be snuggly packed in a 5-μm sperm. (B) In going from the coil to the true discharge (TD), the bundle has to rotate through an angle ø (ø = π in this drawing) at each arm. As the untwisting front propagates along the bundle, it extends out eventually forming zigzag shapes. This unusual design shows how nature uses kinks to convert one form of movement (untwisting) into another (extension). (C) On rare occasions, the second rotation about the z axis does not occur, resulting in a zigzag kinky TD. The arrowhead points the ruptured acrosomal vesicle, which ensures that what we see is the TD coming out of the apical end of the sperm head.

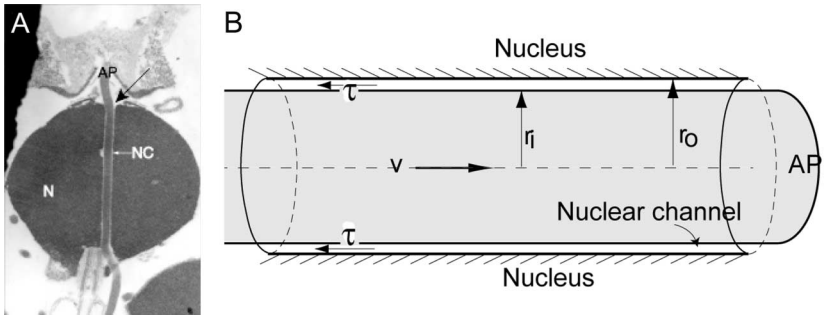

Figure S2. **Hydrodynamic dissipation in the channel.** (A) Thin section electron micrograph of an extending acrosomal bundle shows that the acrosomal process (AP, black arrow) passes through a very tight nuclear channel (NC). (B) The acrosomal bundle moving through a nuclear channel is represented schematically. As the bundle passes through a narrow channel, it experiences a shear force τ . The rate of the hydrodynamic dissipation due to shearing inside the narrow channel can be estimated from $\dot{E} \approx \int \eta(\nabla u)^2 dV$, where η is the viscosity of the cytoplasm (η = 0.01 Pa·s, conservatively estimated to be 10 times that of water); ∇u, the velocity gradient between the nuclear channel wall and the moving acrosome (typically $\nabla u \approx v/[r_o - r_i]$); and V, the volume over which dissipation occurs ($V \approx r_i[r_o - r_i]L$). We calculate the dissipation rate to be 4×10^{-17} W ($10^4\ k_BT/s$), based on the average velocity $v \approx 15$ μm/s, the average bundle radius $r_i \approx 0.05$ μm, the average clearance between the channel and the acrosome, $r_o - r_i \approx 0.005$ μm, and the length of the nuclear channel, $L \approx 5$ μm. For the average duration $t \approx 5$ s, the total energy dissipated is $\dot{E}\, t \approx 10^{-15}$J.

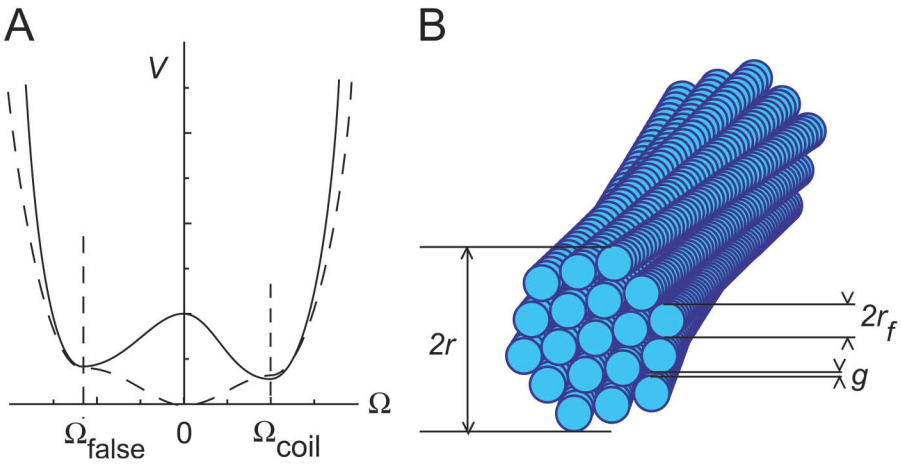

Figure S3. **Theoretical model.** We consider each cross-section of the bundle. Initially, there are two possible stable states of the bundle: the coil and false-discharge states, which have opposite chiralities (A). They are separated by the TD state that is unstable in the absence of calcium, as shown via the solid line in A. Once calcium binds to the scruin–CaM complex, the scruin undergoes a conformation change that causes the actin filaments, originally in their twisted state to be released. Next, the potential well is modified and is converted to the dashed line in A, wherein the TD becomes the globally stable state. This leads to an untwisting of the cross-section, which then propagates as a front along the bundle. To understand the dynamics of this front, we remind ourselves that the driving force is due to the elastic stresses in the twisted bundle, whereas the dissipation is dominated by the shearing between the individual filaments as schematically indicated in B. The balance of twisting torques then leads to the following equation for the twisting strain $\Omega(x,t)$ as a function of location along the bundle x at time t:

$$\alpha\frac{\partial\Omega}{\partial t} = -\left(\frac{\partial V}{\partial\Omega}\right) + \gamma^2\frac{\partial^2\Omega}{\partial x^2},$$

where α is the viscous drag associated with interfilament shearing; γ^2 is the coupling coefficient that penalizes sharp changes in the twist along the bundle; and V is the potential associated with the scruin–actin complex. Looking for traveling wave solutions of the form reduces the equation to a simple ordinary differential equation that can be solved analytically (unpublished data).